Manuscript version: Author's Accepted Manuscript
The version presented in WRAP is the author's accepted manuscript and may differ from the published version or Version of Record.

Persistent WRAP URL:
http://wrap.warwick.ac.uk/111528

How to cite:
Please refer to published version for the most recent bibliographic citation information.
If a published version is known of, the repository item page linked to above, will contain details on accessing it.

Copyright and reuse:
The Warwick Research Archive Portal (WRAP) makes this work by researchers of the University of Warwick available open access under the following conditions.

Copyright © and all moral rights to the version of the paper presented here belong to the individual author(s) and/or other copyright owners. To the extent reasonable and practicable the material made available in WRAP has been checked for eligibility before being made available.

Copies of full items can be used for personal research or study, educational, or not-for-profit purposes without prior permission or charge. Provided that the authors, title and full bibliographic details are credited, a hyperlink and/or URL is given for the original metadata page and the content is not changed in any way.

Publisher's statement:
Please refer to the repository item page, publisher's statement section, for further information.

For more information, please contact the WRAP Team at: wrap@warwick.ac.uk.

warwick.ac.uk/lib-publications

THE DIVERSITY OF KILONOVA EMISSION IN SHORT GAMMA-RAY BURSTS

B. P. Gompertz,[1] A. J. Levan,[1] N. R. Tanvir,[2] J. Hjorth,[3] S. Covino,[4] P. A. Evans,[2] A. S. Fruchter,[5]
C. González-Fernández,[6] Z. P. Jin,[7,8] J. D. Lyman,[1] S. R. Oates,[1] P. T. O'Brien,[2] and K. Wiersema[1]

[1] *Department of Physics, University of Warwick, Coventry, CV4 7AL, UK*

[2] *Department of Physics and Astronomy, University of Leicester, Leicester, LE1 7RH, UK*

[3] *Dark Cosmology Centre, Niels Bohr Institute, University of Copenhagen, Juliane Maries Vej 30, 2100 Copenhagen, Denmark*

[4] *INAF, Osservatorio Astronomico di Brera, Via E. Bianchi 46, I-23807 Merate (LC), Italy*

[5] *Space Telescope Science Institute, 3700 San Martin Drive, Baltimore, MD 21218, USA*

[6] *Institute of Astronomy, University of Cambridge, Madingley Road, Cambridge, CB3 0HA, UK*

[7] *Key Laboratory of dark Matter and Space Astronomy, Purple Mountain Observatory, Chinese Academy of Science, Nanjing, 210008, China*

[8] *School of Astronomy and Space Science, University of Science and Technology of China, Hefei, Anhui 230026, China*

ABSTRACT

The historic first joint detection of both gravitational wave and electromagnetic emission from a binary neutron star merger cemented the association between short gamma-ray bursts (SGRBs) and compact object mergers, as well as providing a well sampled multi-wavelength light curve of a radioactive kilonova (KN) for the first time. Here we compare the optical and near-infrared light curves of this KN, AT2017gfo, to the counterparts of a sample of nearby ($z < 0.5$) SGRBs to characterize their diversity in terms of their brightness distribution. Although at similar epochs AT2017gfo appears fainter than every SGRB-associated KN claimed so far, we find three bursts (GRBs 050509B, 061201 and 080905A) where, if the reported redshifts are correct, deep upper limits rule out the presence of a KN similar to AT2017gfo by several magnitudes. Combined with the properties of previously claimed KNe in SGRBs this suggests considerable diversity in the properties of KN drawn from compact object mergers, despite the similar physical conditions that are expected in many NS-NS mergers. We find that observer angle alone is not able to explain this diversity, which is likely a product of the merger type (NS-NS versus NS-BH) and the detailed properties of the binary (mass ratio, spins etc). Ultimately disentangling these properties should be possible through observations of SGRBs and gravitational wave sources, providing direct measurements of heavy element enrichment throughout the Universe.

Corresponding author: Benjamin Gompertz
b.gompertz@warwick.ac.uk

1. INTRODUCTION

Short gamma-ray bursts (SGRBs) have long been thought to be the products of the mergers of compact objects (Rosswog et al. 2003; Belczynski et al. 2006; Nakar 2007) - either binary neutron star (BNS) or neutron star-black hole (NSBH) systems. In this framework, the energy release of the merger launches relativistic jets that produce γ-rays in internal shocks. A broad-band synchrotron afterglow, with emission ranging from X-ray to radio frequencies, is then produced as the outflow decelerates in the circumstellar environment (Mészáros & Rees 1993). Such a merger is also expected to produce a faint optical/nIR transient known as a 'kilonova' (KN; or 'macronova') (Li & Paczyński 1998; Rosswog 2005; Metzger et al. 2010) as ejected material rich in neutrons forms heavy elements through rapid neutron capture (r-process) nucleosynthesis (Lattimer & Schramm 1974; Eichler et al. 1989; Freiburghaus et al. 1999) that subsequently decay radioactively. However, the discovery of GW 170817 (LIGO Scientific & Virgo Collaboration et al. 2017; LIGO Scientific Collaboration et al. 2017) by the Advanced Laser Interferometer Gravitational-Wave Observatory (LIGO) and Advanced Virgo provided the first direct evidence that the merger of a BNS has occurred. With it came the detection of SGRB 170817A by *Fermi* (Fermi-GBM 2017; Goldstein et al. 2017; von Kienlin et al. 2017) and later INTE-GRAL (Savchenko et al. 2017). In broad-band follow-up observations (LIGO Scientific Collaboration et al. 2017), an optical transient (Coulter 2017a,b; Soares-Santos et al. 2017) identified as a KN, (AT2017gfo; e.g. Cowperthwaite et al. 2017; Chornock et al. 2017; Evans et al. 2017; Nicholl et al. 2017; Pian et al. 2017; Smartt et al. 2017; Tanvir et al. 2017) was detected, thus confirming the compact object merger origin for SGRBs and KNe.

Since 2005, the rapid localisations provided by the *Swift* satellite have meant that a catalogue of SGRB afterglows at multiple wavelengths has been established. These afterglows are at their brightest just after the gamma-ray emission, and decay away in the minutes to days following the burst. Interestingly, in GW 170817 no afterglow was detected after the *Fermi* trigger. Despite being tied to NGC 4993, a nearby early-type galaxy at $z = 0.009783$, or just 42.5 Mpc (Blanchard et al. 2017; Hjorth et al. 2017; Levan et al. 2017), no X-ray emission was detected down to 2.7×10^{-13} erg s^{-1} cm^{-2} at 0.62 days post-trigger (Evans et al. 2017). However, GRB jets are brightest on axis, and are expected to be fainter, and exhibit afterglows which rise later, as the observer moves off-axis. It is therefore tempting to ascribe the faint GRB Fermi-GBM (2017); Goldstein et al. (2017);

von Kienlin et al. (2017), and slowly rising afterglow emission (Troja et al. 2017; Mooley et al. 2018; Lyman et al. 2018; Margutti et al. 2018) to an SGRB viewed away from the axis of its relativistic jet. Indeed, the GW data suggests a viewing angle of up to 28 degrees from the rotation axis of the binary (Evans et al. 2017; Haggard et al. 2017; LIGO Scientific Collaboration et al. 2017; Margutti et al. 2017; Tanvir et al. 2017; Mandel 2018), consistent with an off-axis model. However, the widely adopted simplification of a 'top hat' jet, in which emission drops off sharply outside of narrow beam, likely needs to be modified to include structure away from the core of the jet (e.g. Lazzati et al. 2017). Alternative models featuring emission from a mildly relativistic co-coon of ejecta have also been proposed (e.g. Kasliwal et al. 2017b; Gottlieb et al. 2018; Mooley et al. 2018), though these too may feature a polar jet that could be detected as a more typical cosmological SGRB if it had been oriented towards the Earth.

Due to their typical discovery via detection of the γ-ray jet, SGRBs are normally viewed down the jet axis where the afterglow is brightest and therefore most likely to mask a KN, which is expected to be a more isotropic component, that would normally be easier to see against the glare of the SGRB afterglow at angles away from the SGRB jet (Metzger & Berger 2012). None-the-less, candidate KNe have been observed in just a handful of events: the first and best claim coming with SGRB 130603B (Tanvir et al. 2013; Berger et al. 2013), followed by a re-analysis of SGRBs 060614 (Yang et al. 2015) and 050709 (Jin et al. 2016), and a so far inconclusive fourth candidate in SGRB 160821B (Jin et al. 2017; Kasliwal et al. 2017a).

Through association with BNS mergers and KNe, SGRBs are now thought to be the site of a sizeable fraction of heavy element production in the Universe (Lattimer & Schramm 1974; Rosswog et al. 1998; Goriely et al. 2011; Korobkin et al. 2012; Just et al. 2015), supplementing the apparently insufficient yields predicted for supernovae (Thielemann et al. 2011). The identification of a clear KN signature accompanying GW 170817 and GRB 170817A provides the perfect opportunity to assess their general detectability in SGRBs and the variability in their properties. Known BNS in the Milky Way exist in a rather small range of total mass and mass ratio (Lattimer 2011; Tauris et al. 2017), and so one might naively expect them to drive similar KNe, which therefore ought to be reflected in the SGRB KN population if it is comprised entirely of BNS mergers. Alternatively, it might be that fine differences in the merging binaries or viewer orientation yields strongly

Band	A	t_0	$\tau_{\rm rise}$	$\tau_{\rm fall}$
	μJy	h	h	h
r	544.50	—	—	42.27
y	752.86	11.52	14.05	74.17
J	652.96	24.87	20.00	71.01
K	635.33	58.20	27.21	109.87

Table 1. The best fits for AT2017gfo, taken in the observer frame. The y, J and K-bands are fitted with a Bazin function (Equation 1), while the r-band was better fitted with a simple exponential.

differing observables, or that many SGRBs arise from NSBH rather than BNS mergers.

In this paper, we compare the optical and near-infrared light curves of the KN in GW 170817 to a sample of nearby ($z \lesssim 0.5$) SGRBs to ascertain whether or not a KN of similar magnitude to AT2017gfo could (or even should) have been detected. We use a cosmology of $H_0 = 67.8$ km s^{-1} Mpc^{-1}, $\Omega_M = 0.308$ and $\Omega_\Lambda = 0.692$ (Planck Collaboration et al. 2016) throughout. All reported errors are 1σ, and given upper limits are 3σ.

## 2. AT2017gfo - THE KILONOVA ASSOCIATED WITH GW 170817

Our data for AT2017gfo come from Tanvir et al. (2017). We convert them to absolute magnitudes using a redshift of $z = 0.009783$ (Hjorth et al. 2017; Levan et al. 2017).

To represent the evolution of AT2017gfo, we fit the light curves with Bazin functions (Bazin et al. 2011), which provide an estimate of rise ($\tau_{\rm rise}$) and decay ($\tau_{\rm fall}$) times by fitting the analytical function for a given band

$$f(t) = A \frac{e^{-(t-t_0))/\tau_{\rm fall}}}{1 + e^{-(t-t_0)/\tau_{\rm rise}}}, \qquad (1)$$

where A is the normalisation. Bazin et al. (2011) also present an additive constant, c, which we find to be zero in each case. We therefore re-fit with the constant excluded. Our fits are shown in Figure 1, while the fit parameters are given in Table 1.

These fits demonstrate the strongly chromatic behaviour of AT2017gfo. Indeed, the r-band shows no apparent peak within the span of our data, and declines from ~ 1.5 days as a simple exponential decay. This decay is very different to the power-law seen in GRB afterglows, and coupled with the non-detection of X-rays at comparable times rules out an afterglow component brighter than an r-band absolute magnitude of $M_r \sim -13$ at 0.62 days, assuming the mean r-band to X-ray flux ratio of 1130 found for SGRBs in Nysewander
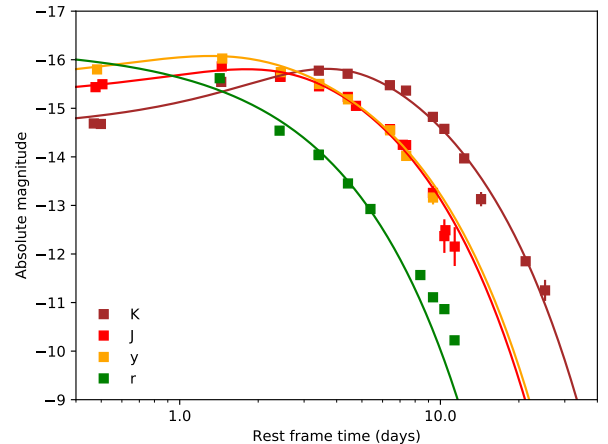
Figure 1. Model fit to AT2017gfo. The y, J and K-bands are fitted with a Bazin function, while the r-band is better fitted with a simple exponential. Error bars are smaller than the plot symbols in most cases.

et al. (2009). Instead, the optical light is probably dominated by a rapidly fading transient created by the synthesis of lanthanide free ejecta, with relatively low opacity (Evans et al. 2017). The redder bands are not well explained by such a simple model, and indeed the light curves appear progressively broader as the observations move redward, and can be explained by a lanthanide-rich, higher opacity component (Tanvir et al. 2017).

3. SGRB DATA SAMPLE

We searched for nearby SGRBs with identified redshifts of $z < 0.5$ in published works (Nysewander et al. 2009; Fong et al. 2015) and unpublished archives.[1] For our sample, we define 'short' GRBs as those with $T_{90} < 2$ s (Kouveliotou et al. 1993), where T_{90} is the duration of the middle 90 per cent of the prompt emission fluence. However, we also include the population of 'extended emission' SGRBs. These bursts exhibit negligible spectral lags and hard spectra within the initial pulse(s) inside 2 s (in common with the SGRB population at large), followed by a softer, low intensity tail that inflates T_{90} to several tens of seconds (Norris & Bonnell 2006; Norris et al. 2010). Our identified sample is shown in Table 2. Optical and IR photometric data are then collected from the published literature, or from GCN circulars. Any Vega magnitudes are converted to AB, and corrections for Galactic absorption are performed following the maps of Schlafly & Finkbeiner (2011) and

---

[1] www.mpe.mpg.de/~jcg/grbgen.html

GRB	z	References	GRB	z	References
050509B	0.2248	1, 2, 3	090515	0.403	28, 29, 30, 31, 32, 33
050709	0.161	4, 5, 6, 7	100206A	0.407	26, 34, 35, 36, 37, 38, 39
050724	0.257	8, 9	100625A	0.452	26, 40, 41, 42
051210	0.114	10, 11	130603B	0.356	43, 44, 45, 46
060502B	0.287	12, 13, 14	140903A	0.351	47
060614	0.125	15	150101B	0.134	48, 49
061006	0.438	16	150120A	0.46	50, 51
061201	0.084	17	150424A	0.3	52, 53, 54, 55, 56
061210	0.41	18, 19, 20	160624A	0.483	57, 58, 59
070724A	0.457	21, 22, 23	160821B	0.16	60, 61
071227	0.384	16, 24, 25, 26	170428A	0.454	62, 63, 64
080905A	0.1218	26, 27	—	—	—

Table 2. The sample of SGRBs with their redshifts, z, and the source of their photometry.
(1) - Castro-Tirado et al. (2005); (2) - Hjorth et al. (2005a); (3) - Bloom et al. (2006); (4) - Fox et al. (2005); (5) - Hjorth et al. (2005b); (6) - Covino et al. (2006); (7) - Jin et al. (2016); (8) - Berger et al. (2005); (9) - Malesani et al. (2007); (10) - Blustin et al. (2005); (11) - Berger & Boss (2005); (12) - Poole & Troja (2006); (13) - Price et al. (2006); (14) - Rumyantsev et al. (2006); (15) - Yang et al. (2015); (16) - D'Avanzo et al. (2009); (17) - Stratta et al. (2007); (18) - Melandri et al. (2006); (19) - Mirabal & Halpern (2006); (20) - Cenko et al. (2006); (21) - Cenko et al. (2007); (22) - Berger et al. (2009); (23) - Kocevski et al. (2010); (24) - D'Avanzo et al. (2007); (25) - Berger et al. (2007); (26) - Nicuesa Guelbenzu et al. (2012); (27) - Rowlinson et al. (2010); (28) - Morgan et al. (2009); (29) - Updike et al. (2009); (30) - Cucchiara et al. (2009); (31) - Siegel & Beardmore (2009); (32) - McLeod & Williams (2009); (33) - Perley et al. (2009); (34) - Leloudas et al. (2010); (35) - Kuroda et al. (2010); (36) - Marshall & Krimm (2010); (37) - Berger & Chornock (2010); (38) - Andreev et al. (2010); (39) - Rumyantsev et al. (2010); (40) - Naito et al. (2010); (41) - Landsman & Holland (2010); (42) - Fong et al. (2013); (43) - Tanvir et al. (2013); (44) - Cucchiara et al. (2013); (45) - de Ugarte Postigo et al. (2014); (46) - Fong et al. (2014); (47) - Troja et al. (2016a); (48) - D'Avanzo et al. (2015); (49) - Fong et al. (2016); (50) - Chornock & Fong (2015); (51) - Chester & D'Elia (2015); (52) - Marshall & Beardmore (2015); (53) - Malesani et al. (2015); (54) - Kann et al. (2015); (55) - Butler et al. (2015); (56) - Knust et al. (2017); (57) - Kuroda et al. (2016); (58) - Kong et al. (2016); (59) - de Pasquale & D'Ai (2016); (60) - Jin et al. (2017); (61) - Kasliwal et al. (2017a); (62) - Kuin & Beardmore (2017); (63) - Bolmer et al. (2017); (64) - Troja et al. (2017).

using $R_v = 3.1$ for the Milky Way. We do not make any corrections for extinction in the SGRB host galaxies.

In AT2017gfo it appears that the optical and IR light is dominated by the KN, at least for several days after the merger, and possibly for longer. Any afterglow component is very weak (Evans et al. 2017). However, in SGRBs the situation is very different. It is likely that most SGRBs are viewed close to the jet axis (see e.g. Ryan et al. 2015), and so show X-ray and optical afterglows. These afterglows probably dominate the light, at least for the first several days after the merger. However, the early, bright blue and UV emission from AT2017gfo also suggests that such KN may contribute here. Therefore, it is desirable to estimate the likely afterglow contribution in the optical bands at these times. SGRB afterglows are well established as synchrotron phenomena, and so the X-ray data can be fairly simply extrapolated to optical frequencies. This provides a baseline estimate for the expected magnitude of the afterglow, which can be compared to the optical/nIR observations to check

for any excesses that may be symptomatic of a KN (see the shaded regions in Figure 2), although it suffers from limitations due to the large lever-arm between X-ray and optical frequencies, over which the errors associated with the X-ray observations become significant.

Swift X-Ray Telescope (XRT) data are obtained for each SGRB from the 1 keV flux density light curves on the UK *Swift* Science Data Centre (UKSSDC) burst analyser[2] (Evans et al. 2007, 2009), except for SGRB 150101B, where we take the *Chandra* data from Fong et al. (2016) because the *Swift* light curve is dominated by the Active Galactic Nucleus (AGN) in the host galaxy. Additional X-ray data from *Chandra* and/or XMM-*Newton* are added for SGRBs 050709 (Fox et al. 2005), 050724 (Grupe et al. 2006), 130603B (Fong et al. 2014) and 140903A (Troja et al. 2016a). We correct the *Swift* data for absorption using a ratio of [counts-

---

[2] www.swift.ac.uk/burst_analyser/

to-flux unabsorbed]/[counts-to-flux observed], which we obtain from the automatically generated late-time photon counting mode spectral fit in the XRT spectrum repository on the UKSSDC website. The flux densities are converted to AB magnitudes and extrapolated to 6260Å (r-band) for easy comparison with the optical data. The assumed spectral indices of the extrapolation are $\beta = 0.5$, which represents the case in which the synchrotron cooling break is above the X-ray frequency, and $\beta = 1.0$, which implies the synchrotron cooling break is down near optical frequencies. Both of these assume that the electron energies follow a power-law distribution with an index of $p = 2$, which is the theoretically expected value (Sari et al. 1998). In nature, measurements of spectral and temporal indices often imply that this distribution is steeper than $p = 2$ (e.g. Curran et al. 2010), suggesting that a steeper spectral index would be needed. However, the synchrotron cooling break is typically measured to be somewhere close to X-ray frequencies rather than in the optical part of the spectrum (e.g. Gompertz et al. 2015), so flux densities bracketed by our two extrapolations provide a reasonable estimation of where the SGRB afterglow should occur.

We convert all apparent magnitudes to absolute magnitudes, assuming for a given band k, $k_{abs} = k_{AB} - 5 \log_{10}(d_L/10\text{pc}) + 2.5 \log_{10}(1 + z)$. Observed times are divided by $(1 + z)$ to put them in the rest frame. We do not correct for the redshift of the central frequency of the photometric filter because this would require assuming a spectral shape that is uncertain in many SGRBs. Instead we interpolate and shift the well sampled lightcurve of AT2017gfo to the rest frame wavelength represented by the observations (see below). This means our photometry is presented in its observer frame band, such that the magnitudes are given at $\lambda_k = (1 + z)\lambda_r$, where λ_r is the rest frame emitting wavelength. Since KNe do not appear (or are at least very weak) at X-ray frequencies, this issue does not affect our X-ray extrapolations.

While the optical to IR spectral energy distributions of our SGRBs are usually poorly constrained, we do have good colour coverage of AT2017gfo. We therefore adjust our model fits to the wavelengths of the SGRB observations via linear interpolations between the fitted curves in Figure 1. Where the rest-frame frequency is bluewards of the r-band fit to AT2017gfo, we supplement with observations with the *Swift*-UVOT u-band data from Evans et al. (2017) and the HST F475W (g-band) data from Tanvir et al. (2017), with an early g-band point based on the spectral flux density measured in our MUSE spectroscopy. We fit both

datasets with an exponential decay to ascertain the required colour correction. Fitting in the observer frame, we find $A_g = 321.92\ \mu$Jy, $\tau_{g,fall} = 39.10$ hours, and $A_u = 321.39\ \mu$Jy, $\tau_{u,fall} = 20.25$ hours. We note that these bands have only a small number (3-4) points to fit, and so we have assumed they follow an exponential decay as the r-band does, but do not have sufficient data discriminate between alternative models. We do not extrapolate beyond the u-band if the rest-frame wavelength is less than 3560Å.

4. RESULTS

Light curves of our results are shown in Figure 2. Based on these light curves, our sample broadly divides into four main categories:

1. SGRBs with deep limits constraining to an AT2017gfo-like KN.

2. SGRBs with candidate KNe.

3. SGRBs with afterglow detections bright enough to mask an AT2017gfo-like KN.

4. SGRBs with no constraining observations.

4.1. *SGRBs with deeper limits than AT2017gfo*

We find that for several SGRBs, a KN as bright as AT2017gfo could have been detected. For four bursts in particular, deep 3σ upper limits that a factor of two or more fainter than the detections of AT2017gfo at comparable rest-frame times appear to rule out a KN like AT2017gfo. They are SGRBs 050509B (3 times fainter than AT2017gfo), 051210 (2 times fainter), 061201 (4 times fainter) and 080905A (4.5 times fainter).

In each case, a KN similar to AT2017gfo could have been detected if it had been present. These limits assume that in each case the redshift of the burst is correctly ascribed, and this is considered in more detail in Section 5. It should also be noted again that no host galaxy extinction has been included in our study.

4.2. *SGRBs with candidate KNe*

Compared to the SGRB KN candidates, AT2017gfo appears to be faint, though the contribution of the SGRB afterglow to the observed flux in the bursts is uncertain. The H-band detection in GRB 130603B is almost 3 times brighter than the interpolated KN model fit at the time of the observation. Similarly in SGRB 050709, the K-band detection is far brighter than the K-band of AT2017gfo. However, the i-band light curve appears to be fainter and peak later, though the photometry is limited. The afterglow of GRB 060614 is already much brighter than the light curve of AT2017gfo,
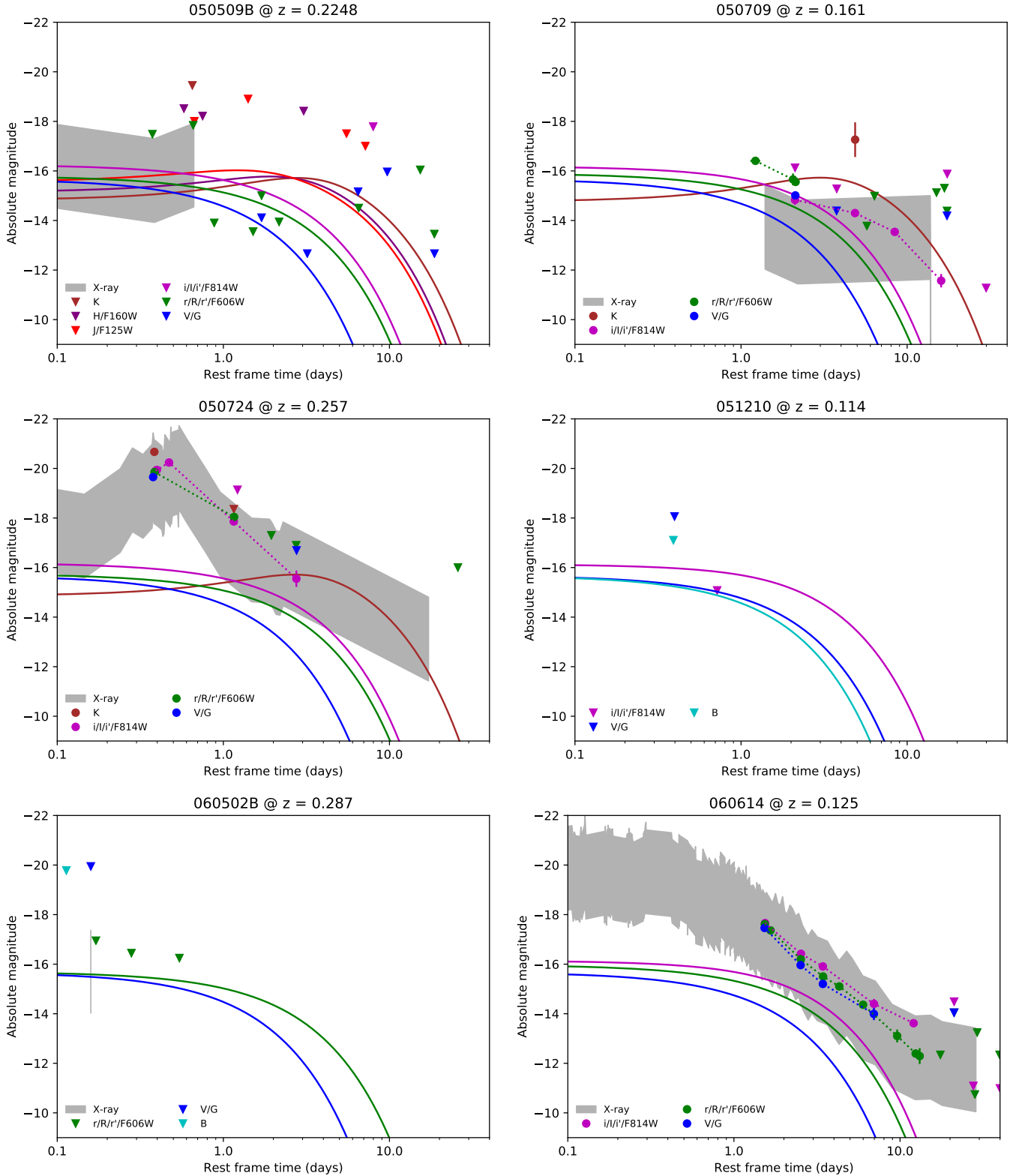
Figure 2. Our sample of SGRB afterglows compared to the model fits of AT2017gfo. Coloured circles are detections, and triangles are upper limits. These data are presented in their observer frame filters, and the AT2017gfo models (coloured lines) are shifted in frequency to match them using linear interpolation of the fits in Figure 1 supplemented by the g-band data from Tanvir et al. (2017) and the u-band data from Evans et al. (2017). We do not extrapolate if the rest-frame wavelength is below the u-band (3560Å), so some data do not have models plotted. The grey band is the extrapolation of the X-ray flux to 6260Å (r-band). SGRBs from Table 2 with no constraining observations are not included.
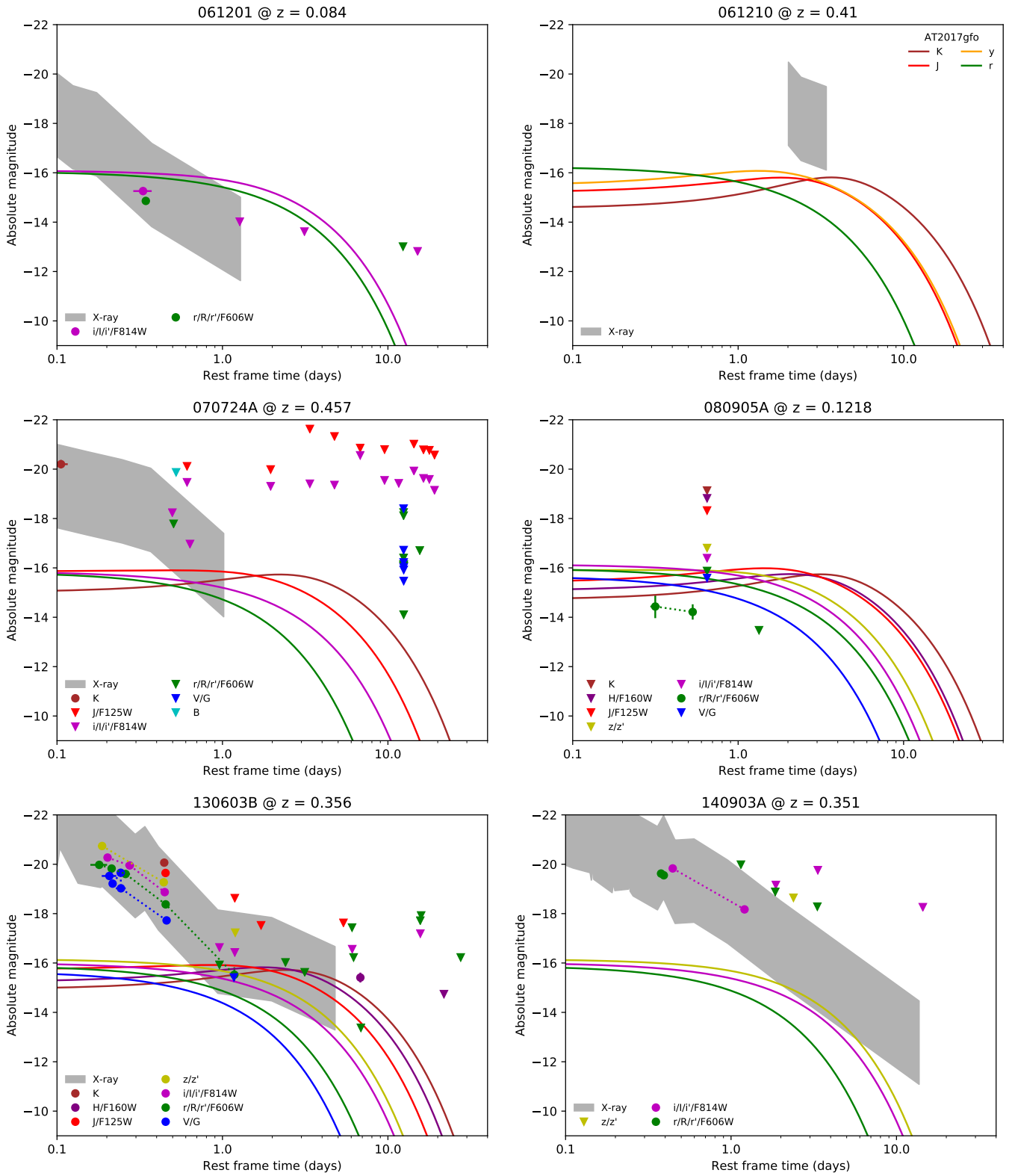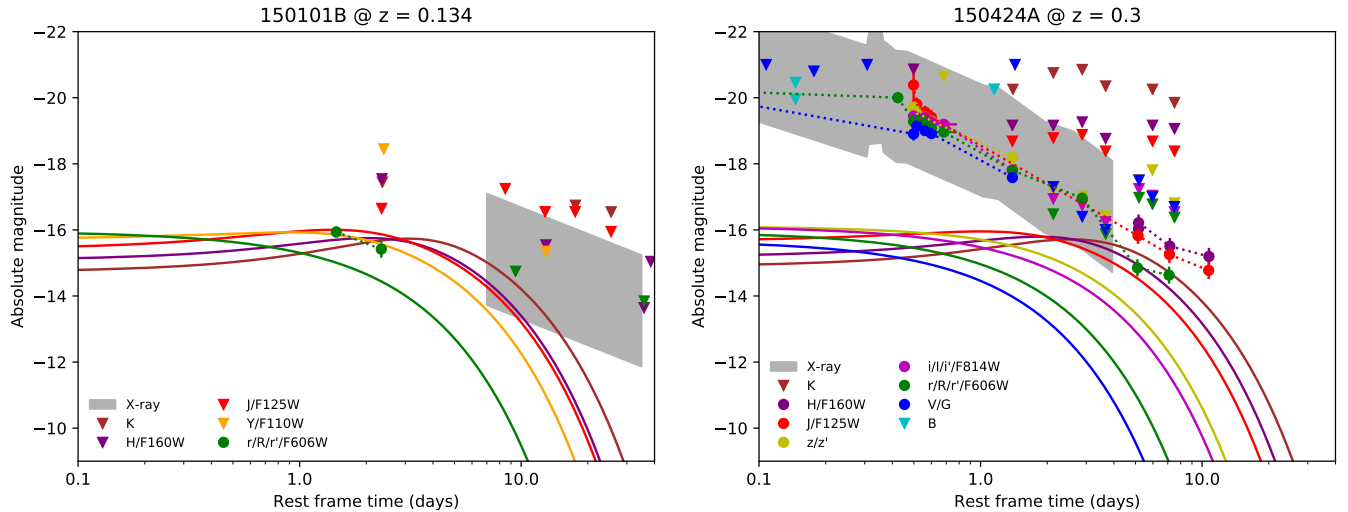
Figure 2. continued

Figure 2. continued

and the i-band photometric excess (Yang et al. 2015) is over 50 times brighter than the contemporary KN fit, though it could be a later/longer rise like SGRB 050709. Alternatively, as shown in Figure 2, the extrapolation of the X-ray afterglow to optical/IR wavelengths may imply significant afterglow contributions at this time, such that the KN components can be fainter. The photometric excess claimed by Jin et al. (2017) in 160821B is the only potential KN less bright than AT2017gfo (see Troja et al. 2016b), though the data are inconclusive in this case (see Tanvir et al. in prep. for a detailed analysis of this burst).

4.3. *SGRBs with bright afterglows*

We identify several SGRBs in which the afterglow was likely too bright for a AT2017gfo-like KN to be detected. SGRB 150424A has optical/nIR afterglow detections several magnitudes brighter than AT2017gfo (see Tanvir et al. 2015), and its detections and limits are never less than about 3 times brighter than the relevant model light curve in the H-band, or 10 times in the r-band. This burst may also be at a higher redshift than reported here (Tanvir et al. 2015), which would mean the afterglow is even brighter when corrected for distance. SGRBs 140903A and 150101B both have extrapolated X-ray afterglows that are brighter than AT2017gfo, with optical detections that support the extrapolation, though there are no nIR limits constraining a redder transient. The i-band detection in SGRB 140903A is almost 15 times brighter than the AT2017gfo model. The r-band detection in SGRB 150101B is just 2 times the flux of the AT2017gfo model, so could potentially have a KN contribution. It is notable that its decay between the two epochs of observations is very simiar

to AT2017gfo. SGRB 050724 features a large flare seen in X-ray, nIR and optical bands. The i-band detection close to 3 days is of a similar brightness to the one in 060614 (which was identified as a KN by its i-band excess; Yang et al. 2015), but the contribution from the various emission features is unknown.

4.4. *SGRBs with no constraining observations*

In the final category, six SGRBs do not have sufficiently deep observations to place any meaningful constraints on the presence of a KN like AT2017gfo.

SGRB 061210 may potentially have a bright afterglow if the extrapolated X-ray flux is in fact representative, but no observations in the optical/nIR are available. Neither SGRB 070724A nor 060502B have optical or nIR limits deep enough to provide meaningful constraints on the AT2017gfo models. However, the r-band limits in 060502B are within a factor of 2 of the r-band model of AT2017gfo, suggesting that any KN in this burst is not significantly brighter than AT2017gfo. SGRBs 061006, 071227 and 170428A all lie on bright host galaxies. No image subtraction of the host galaxy has been performed, and so any contributions from the afterglow or a possible KN are swamped by the light of the host.

4.5. *Colours*

One of the more distinct features of AT2017gfo was its colour evolution. The optical transient began blue, and slowly became redder over the course of several days (see e.g. Figure 3 from Tanvir et al. 2017). This was explained as a two (or possibly three) component KN: a 'blue' component from high velocity lanthanide-poor dynamical ejecta from the poles (e.g. Nicholl et al. 2017),

and a slower 'red' lanthanide-rich component driven in an isotropic wind, and rising to prominence later. Some groups also invoke an intermediate 'purple' component (e.g. Villar et al. 2017).

Many of the SGRBs in our sample feature multi-colour detections, and this allows us to compare their colours to AT2017gfo. Seven feature photometric detections in more than one filter that are approximately contemporaneous. They are SGRBs 050709, 050724, 060614, 061201, 130603B, 140903A and 150424A. We compare their colours to our model curves of AT2017gfo. Colours are compared in the rest frame, and so are k-corrected from their initial redshift.

From the KN candidates, SGRB 050709 appears to be bluer than AT2017gfo at around 2 rest-frame days after trigger when measured in g-r (0.55 ± 0.12 in the SGRB data versus ~ 0.96 in our AT2017gfo model) and r-i (-0.30 ± 0.22 versus ~ 0.50). However, at around 5 days after trigger its I-K colour of 2.96 ± 0.70 is comparable within errors to our model fits, where I-K ~ 2.12. Whether this is due to colour evolution is uncertain because we have no K band magnitude measurements from the earlier epoch. At 2 days, SGRB 050709 is brighter in r than in either g or i. This is unusual for an SGRB afterglow, and potentially suggests some spectral evolution. SGRB 060614 is also bluer than AT2017gfo early on, with g-r = 0.15 ± 0.04 in the data compared to ~ 0.74 in the model, and r-i = 0.05 ± 0.04 in the data versus ~ 0.42 in the model at around 1.5 rest-frame days. It shows a redwards linear evolution in both colours in a similar way to AT2017gfo, becoming g-r = 0.30 ± 0.10 (~ 1.31) and r-i = 0.41 ± 0.11 (~ 0.56) over the next two days. By 2 weeks after trigger, the colours have converged, with r-i = 1.23 ± 0.18 in the data and r-i ~ 1.11 in the model. This may indicate that the KN in 060614 now dominates the observed emission. Multi-wavelength coverage for SGRB 130603B is only available inside one day after trigger. This emission has already been shown to be consistent with an afterglow by Fong et al. (2014). The r-i colour is 0.45 ± 0.06, compared to ~ 0.19 for the contemporaneous AT2017gfo model at 0.2 days.

At almost half a day after trigger, the r-i colour of the model is ~ 0.25, and three of the remaining four SGRBs with colour information are broadly consistent with this: 061201 has r-i 0.40 ± 0.14; 140903A has r-i = 0.28 ± 0.08; and 150424A has r-i = 0.16 ± 0.14. The exception, 050724, exhibits a large flare at this time (Figure 2). There is no evidence for significant evolution beyond this time, in most cases due to a lack of continuing multi-colour monitoring. SGRB 150424A has r-i = 0.01 ± 0.15 at 1.4 days, consistent with no evolution, while the

AT2017gfo model has evolved to r-i ~ 0.65 at this time. Jin et al. (2017) also found this SGRB to be consistent with no chromatic evolution.

5. DISCUSSION

We search our sample of 23 SGRBs with identified redshift of $z < 0.5$ and optical/nIR observations for detections and limits constraining to KNe similar to AT2017gfo, or bright afterglows capable of masking a KN of this magnitude. 3 have claimed KNe in the literature (050709, 060614, 130603B) with a further marginal case (160821B; see Tanvir et al. in prep. for a detailed analysis). 4 have limits deeper than AT2017gfo (050509B, 051210, 061201, 080905A), and 3 of these are over a magnitude deeper (050509B, 061201, 080905A). 1 more has limits of comparable depth (060502B). 4 have bright optical/nIR detections consistent with light arising from an afterglow component (050724, 140903A, 150101B, 150424A), although at least in one case at magnitudes only marginally brighter than AT2017gfo (GRB 150101B). 2 have afterglows that are implied to be bright by the X-ray extrapolation (061210, 070724A), although were in fact not observed (in the case of 070724A, the absence of the afterglow has been suggested to be due to the presence of dust; Berger et al. 2009). 3 have bright host galaxies (061006, 071227, 170428A), and the remaining 5 are completely unconstrained by the available observations. The broad range of magnitudes in the sample suggests a diversity in the brightness of KNe associated with SGRBs.

For three bursts in particular, the absence of a KN is conspicuous. SGRBs 050509B, 061201 and 080905A all have limits much deeper than the detections for AT2017gfo, and any KN would have had to have been at least five times fainter to be missed, yet AT2017gfo itself is fainter than any KN seen in SGRBs so far. Our findings for SGRB 050509B are consistent with Fong et al. (2017).

There are two concerns that should be addressed in interpreting these limits. The first is whether there could be some unseen extinction along the line of sight. In the case of SGRB 050509B and 051210 this is of particular concern because there is no optical light at any epoch, and too few X-ray photons to determine a column density. However, SGRB 050509B is spatially coincident with the outskirts of a giant elliptical galaxy (Castro-Tirado et al. 2005; Gehrels et al. 2005; Hjorth et al. 2005b; Bloom et al. 2006), which is the putative host (and the source of the redshift). Given its location, it is unlikely that dust extinction plays a significant role. The apparent faintness of the optical/nIR emission is therefore more likely to be intrinsic, perhaps due to a

sparse local environment or a wide viewing angle from the SGRB jet. For SGRB 061201 and 080905A the detection of the sources in optical light rules out extreme extinction, but does not discount moderate levels. Fong et al. (2015) find that both of these bursts are consistent with having no host extinction in their modelling, and this suggests that the limits on a KN are indeed as constraining as they appear to be. It is notable in these examples that the optical light is consistent with the X-ray extrapolation (where available) with $\beta = 0.5$, and so the bursts are not "dark" GRBs (Jakobsson et al. 2004).

The second concern is the validity of the assumed redshifts. Only one short GRB has a redshift measured in absorption, GRB 130603B (de Ugarte Postigo et al. 2014). In other cases the redshifts are based on putative host galaxy identifications. For GRB 050509B there is a large cD galaxy close to the location, and a coincidence with a massive, merging galaxy cluster. Much of the mass along this line of sight lies within this cluster, and the redshift has high confidence (see e.g. Bloom et al. 2002; Levan et al. 2007). For GRB 080905A the burst position overlaps the spiral arm of the host galaxy, again suggesting a chance alignment probability of $\lesssim 1\%$. However, for GRB 061201 the situation is more complex. The burst belongs to the so-called hostless SGRB population (Berger 2010; Tunnicliffe et al. 2014), and so the redshift is based on a proximity to the Abell 995 cluster (Berger 2006; Stratta et al. 2007). This is a rich cluster, but there are no galaxies within a few arcseconds of the burst position, and so the probability of chance a alignment is significant, and the redshift should be viewed with caution. While the probabilities of any given burst redshift being wrong appear small, it should also be noted that assigning redshifts by probabilistic arguments favours the brightest nearby galaxies, many of which are likely to be closer, and so this may produce a bias in which incorrect host assignments, lead to lower redshifts, and hence strong KN constraints.

The SGRBs with bright afterglows still may have KN contributions in the detected flux. The inferred contribution from an AT2017gfo-like KN ranges from 1/15 (140903A, i-band) to 1/2.5 (150101B, r-band), and the latter end of the scale is certainly enough to cause a spectral energy distribution (SED) to deviate away from the power law expected from the synchrotron afterglow. A KN was discovered this way for both SGRBs 050709 (Jin et al. 2016) and 060614 (Yang et al. 2015), and potentially 160821B too (Jin et al. 2017). However, no multi-colour observations are available for any of these bursts except 150424A, the brightest of the four. Jin et al. (2017) found no evidence of chromatic deviation in this source.

AT2017gfo appears to be somewhat fainter than other established KN, but the lack of X-ray afterglow to deep limits (2.7×10^{-13} erg s^{-1} cm^{-2} at 0.62 days after trigger; Evans et al. 2017) and constraints from the GW data suggest that the viewing angle is further off-axis than in typical SGRBs - perhaps up to 28 degrees away from the jet axis (Evans et al. 2017; Haggard et al. 2017; LIGO Scientific Collaboration et al. 2017; Margutti et al. 2017; Tanvir et al. 2017). The fainter KN in GW 170817 is therefore within the variation expected from the observer position (e.g. Grossman et al. 2014). The peak time and luminosity of a KN is also a function of ejecta mass and opacity (e.g. Metzger et al. 2010), and naturally some variation is expected from case to case.

6. CONCLUSIONS

Our analysis reveals a diverse range of KN possibilities, as in some SGRBs we find upper limits for optical/nIR emission several magnitudes deeper than AT2017gfo, in others there are identified (or suspected) KNe that are brighter, and we also find SGRBs with bright afterglows capable of masking KNe that are brighter still. Our sample spans five magnitudes at a few days after trigger (Figure 3). The most interesting comparison is between the SGRBs with detected KNe (including AT2017gfo) and the 3 SGRBs with deep limits; the diversity between these two groups is hard to reconcile with the highly uniform distribution of known BNS masses and mass ratios in the Milky Way (Lattimer 2011; Tauris et al. 2017).

The relatively small range of viewing angles in the SGRB population means that the observer position alone probably can't explain the ~ 3.5 magnitudes (a factor of 25 in flux) between the KN in SGRB 060614 and the upper limits in SGRBs 061201 and 080905A. If their redshifts are correct, they may potentially suggest a BNS/NSBH dichotomy in the SGRB population, as this represents the most natural way to explain an apparent contrast in the ejected masses available to power a KN; an NSBH merger can produce as much as 10 times more dynamical ejecta than can a BNS (Metzger 2017).

The LIGO/Virgo detection of GW 170817 and electromagnetic follow-up and identification of SGRB 170717A and AT2017gfo brings about the advent of KN astronomy. Further observations of KNe will reveal whether the magnitude of the emission forms a continuum, or continues to display a gap in brightness between two populations. Unsurprisingly, our best constraints come from the SGRBs at the lowest redshifts, and our work emphasises the need to perform KN searches at low z and in nIR filters.
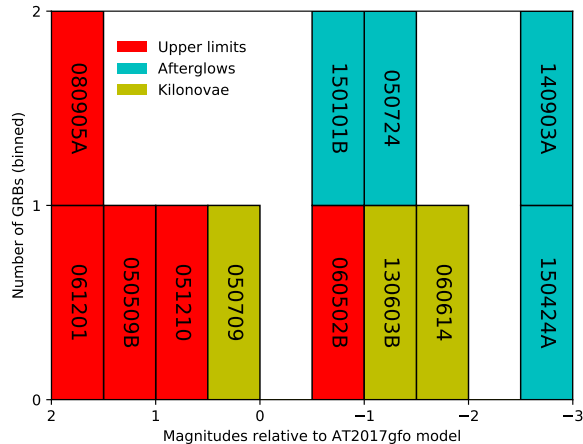
Figure 3. A snapshot of the i/r-band magnitudes of our SGRB observations relative to the AT2017gfo models, taken between 0.5 and 3 days after trigger. Data are binned into 0.5 magnitude intervals. Bursts with data not constraining to the AT2017gfo models are not included. 'Upper limits' (red) refers to bursts with deep limits constraining to an AT2017gfo-like KN. 'Afterglows' (blue) are the SGRBs with afterglows bright enough to mask AT2017gfo. 'Kilonovae' (yellow) are the SGRB KN candidates.

REFERENCES

Andreev, M., Sergeev, A., Parakhin, N., et al. 2010, GRB Coordinates Network, Circular Service, No. 10455, #1 (2010), 10455

Bazin, G., Ruhlmann-Kleider, V., Palanque-Delabrouille, N., et al. 2011, A&A, 534, A43

Belczynski, K., Perna, R., Bulik, T., et al. 2006, ApJ, 648, 1110

Berger, E. 2006, GRB Coordinates Network, 5952

—. 2010, ApJ, 722, 1946

Berger, E., & Boss, A. 2005, GRB Coordinates Network, 4323

Berger, E., Cenko, S. B., Fox, D. B., & Cucchiara, A. 2009, ApJ, 704, 877

Berger, E., & Chornock, R. 2010, GRB Coordinates Network, Circular Service, No. 10410, #1 (2010), 10410

Berger, E., Fong, W., & Chornock, R. 2013, ApJL, 774, L23

Berger, E., Morrell, N., & Roth, M. 2007, GRB Coordinates Network, 7151

Berger, E., Price, P. A., Cenko, S. B., et al. 2005, Nature, 438, 988

Blanchard, P. K., Berger, E., Fong, W., et al. 2017, ApJL, 848, L22

Bloom, J. S., Kulkarni, S. R., & Djorgovski, S. G. 2002, AJ, 123, 1111

Bloom, J. S., Prochaska, J. X., Pooley, D., et al. 2006, ApJ, 638, 354

Blustin, A. J., Mangano, V., Voges, W., Marshall, F., & Gehrels, N. 2005, GRB Coordinates Network, 4331

Bolmer, J., Steinle, H., & Schady, P. 2017, GRB Coordinates Network, Circular Service, No. 21050, #1 (2017), 21050

Butler, N., Watson, A. M., Kutyrev, A., et al. 2015, GRB Coordinates Network, Circular Service, No. 17762, #1 (2015), 17762

Castro-Tirado, A. J., de Ugarte Postigo, A., Gorosabel, J., et al. 2005, A&A, 439, L15

Cenko, S. B., Fox, D. B., & Price, P. A. 2006, GRB Coordinates Network, 5912

Cenko, S. B., Rau, A., Berger, E., Price, P. A., & Cucchiara, A. 2007, GRB Coordinates Network, 6664

Chester, M. M., & D'Elia, V. 2015, GRB Coordinates Network, Circular Service, No. 17323, #1 (2015), 17323

Chornock, R., & Fong, W. 2015, GRB Coordinates Network, Circular Service, No. 17358, #1 (2015), 17358

Chornock, R., Berger, E., Kasen, D., et al. 2017, ApJL, 848, L19

Coulter, D. A. e. a. 2017a, GRB Coordinates Network, 21529

—. 2017b, Science, doi:10.1126/science.aap9811

Covino, S., Malesani, D., Israel, G. L., et al. 2006, A&A, 447, L5

Cowperthwaite, P. S., Berger, E., Villar, V. A., et al. 2017, ApJL, 848, L17

Cucchiara, A., Fox, D. B., Tanvir, N., et al. 2009, GRB Coordinates Network, 9362

Cucchiara, A., Prochaska, J. X., Perley, D., et al. 2013, ApJ, 777, 94

Curran, P. A., Evans, P. A., de Pasquale, M., Page, M. J., & van der Horst, A. J. 2010, ApJL, 716, L135

D'Avanzo, P., D'Elia, V., Lorenzi, V., et al. 2015, GRB Coordinates Network, Circular Service, No. 17326, #1 (2015), 17326

D'Avanzo, P., Piranomonte, S., Antonelli, L. A., et al. 2007, GRB Coordinates Network, 7149

D'Avanzo, P., Malesani, D., Covino, S., et al. 2009, A&A, 498, 711

de Pasquale, M., & D'Ai, A. 2016, GRB Coordinates Network, Circular Service, No. 19576, #1 (2016), 19576

de Ugarte Postigo, A., Thöne, C. C., Rowlinson, A., et al. 2014, A&A, 563, A62

Eichler, D., Livio, M., Piran, T., & Schramm, D. N. 1989, Nature, 340, 126

Evans, P. A., Cenko, S. B., Kennea, J. A., et al. 2017, doi:10.1126/science.aap9580

Evans, P. A., Beardmore, A. P., Page, K. L., et al. 2007, A&A, 469, 379

—. 2009, MNRAS, 397, 1177

Fermi-GBM. 2017, GRB Coordinates Network, 524666471

Fong, W., Berger, E., Margutti, R., & Zauderer, B. A. 2015, ApJ, 815, 102

Fong, W., Berger, E., Chornock, R., et al. 2013, ApJ, 769, 56

Fong, W., Berger, E., Metzger, B. D., et al. 2014, ApJ, 780, 118

Fong, W., Margutti, R., Chornock, R., et al. 2016, ApJ, 833, 151

Fong, W., Berger, E., Blanchard, P. K., et al. 2017, ApJL, 848, L23

Fox, D. B., Frail, D. A., Price, P. A., et al. 2005, Nature, 437, 845

Freiburghaus, C., Rosswog, S., & Thielemann, F.-K. 1999, ApJL, 525, L121

Gehrels, N., Sarazin, C. L., O'Brien, P. T., et al. 2005, Nature, 437, 851

Goldstein, A., Veres, P., Burns, E., et al. 2017, ApJL, 848, L14

Gompertz, B. P., van der Horst, A. J., O'Brien, P. T., Wynn, G. A., & Wiersema, K. 2015, MNRAS, 448, 629

Goriely, S., Bauswein, A., & Janka, H.-T. 2011, ApJL, 738, L32

Gottlieb, O., Nakar, E., & Piran, T. 2018, MNRAS, 473, 576

Grossman, D., Korobkin, O., Rosswog, S., & Piran, T. 2014, MNRAS, 439, 757

Grupe, D., Burrows, D. N., Patel, S. K., et al. 2006, ApJ, 653, 462

Haggard, D., Nynka, M., Ruan, J. J., et al. 2017, ApJL, 848, L25

Hjorth, J., Levan, A. J., Tanvir, N. R., et al. 2017, ApJL, doi:10.3847/2041-8213/aa9110

Hjorth, J., Sollerman, J., Gorosabel, J., et al. 2005a, ApJL, 630, L117

Hjorth, J., Watson, D., Fynbo, J. P. U., et al. 2005b, Nature, 437, 859

Jakobsson, P., Hjorth, J., Fynbo, J. P. U., et al. 2004, ApJL, 617, L21

Jin, Z.-P., Hotokezaka, K., Li, X., et al. 2016, Nature Communications, 7, 12898

Jin, Z.-P., Li, X., Wang, H., et al. 2017, ArXiv e-prints, arXiv:1708.07008

Just, O., Bauswein, A., Pulpillo, R. A., Goriely, S., & Janka, H.-T. 2015, MNRAS, 448, 541

Kann, D. A., Tanga, M., & Greiner, J. 2015, GRB Coordinates Network, Circular Service, No. 17757, #1 (2015), 17757

Kasliwal, M. M., Korobkin, O., Lau, R. M., Wollaeger, R., & Fryer, C. L. 2017a, ApJL, 843, L34

Kasliwal, M. M., Nakar, E., Singer, L. P., et al. 2017b, Science, 358, 1559

Knust, F., Greiner, J., van Eerten, H. J., et al. 2017, A&A, 607, A84

Kocevski, D., Thöne, C. C., Ramirez-Ruiz, E., et al. 2010, MNRAS, 404, 963

Kong, A. K. H., Lee, M. Y., Lin, Y.-M., Hou, X., & Liu, C. Y. 2016, GRB Coordinates Network, Circular Service, No. 19575, #1 (2016), 19575

Korobkin, O., Rosswog, S., Arcones, A., & Winteler, C. 2012, MNRAS, 426, 1940

Kouveliotou, C., Meegan, C. A., Fishman, G. J., et al. 1993, ApJL, 413, L101

Kuin, N. P. M., & Beardmore, A. P. 2017, GRB Coordinates Network, Circular Service, No. 21049, #1 (2017), 21049

Kuroda, D., Yanagisawa, K., Shimizu, Y., et al. 2010, GRB Coordinates Network, Circular Service, No. 10388, #1 (2010), 10388

Kuroda, D., Hanayama, H., Miyaji, T., et al. 2016, GRB Coordinates Network, Circular Service, No. 19571, #1 (2016), 19571

Landsman, W., & Holland, S. 2010, GRB Coordinates Network, Circular Service, No. 10892, #1 (2010), 10892

Lattimer, J. M. 2011, Ap&SS, 336, 67

Lattimer, J. M., & Schramm, D. N. 1974, ApJL, 192, L145

Lazzati, D., Perna, R., Morsony, B. J., et al. 2017, ArXiv e-prints, arXiv:1712.03237

Leloudas, G., Xu, D., Malesani, D., et al. 2010, GRB Coordinates Network, Circular Service, No. 10387, #1 (2010), 10387

Levan, A. J., Jakobsson, P., Hurkett, C., et al. 2007, MNRAS, 378, 1439

Levan, A. J., Lyman, J. D., Tanvir, N. R., et al. 2017, ApJL, 848, L28

Li, L.-X., & Paczyński, B. 1998, ApJL, 507, L59

LIGO Scientific, & Virgo Collaboration et al. 2017, GRB Coordinates Network, 21505

LIGO Scientific Collaboration, Virgo Collaboration, & Partner Astronomy Groups. 2017, doi:10.1103/PhysRevLett.119.161101

Lyman, J. D., Lamb, G. P., Levan, A. J., et al. 2018, ArXiv e-prints, arXiv:1801.02669

Malesani, D., Xu, D., Watson, D. J., & Blay, P. 2015, GRB Coordinates Network, Circular Service, No. 17756, #1 (2015), 17756

Malesani, D., Covino, S., D'Avanzo, P., et al. 2007, A&A, 473, 77

Mandel, I. 2018, ApJL, 853, L12

Margutti, R., Berger, E., Fong, W., et al. 2017, ApJL, 848, L20

Margutti, R., Alexander, K. D., Xie, X., et al. 2018, ArXiv e-prints, arXiv:1801.03531

Marshall, F. E., & Beardmore, A. P. 2015, GRB Coordinates Network, Circular Service, No. 17751, #1 (2015), 17751

Marshall, F. E., & Krimm, H. A. 2010, GRB Coordinates Network, Circular Service, No. 10394, #1 (2010), 10394

McLeod, B., & Williams, G. 2009, GRB Coordinates Network, 9370

Melandri, A., Carter, D., Mundell, C., et al. 2006, GRB Coordinates Network, 5920

Mészáros, P., & Rees, M. J. 1993, ApJ, 405, 278

Metzger, B. D. 2017, Living Reviews in Relativity, 20, 3

Metzger, B. D., & Berger, E. 2012, ApJ, 746, 48

Metzger, B. D., Martínez-Pinedo, G., Darbha, S., et al. 2010, MNRAS, 406, 2650

Mirabal, N., & Halpern, J. P. 2006, GRB Coordinates Network, 5906

Mooley, K. P., Nakar, E., Hotokezaka, K., et al. 2018, Nature, 554, 207

Morgan, A. N., Cobb, B. E., Klein, C., & Bloom, J. S. 2009, GRB Coordinates Network, 9359

Naito, H., Sako, T., Suzuki, D., et al. 2010, GRB Coordinates Network, Circular Service, No. 10889, #1 (2010), 10889

Nakar, E. 2007, PhR, 442, 166

Nicholl, M., Berger, E., Kasen, D., et al. 2017, ApJL, 848, L18

Nicuesa Guelbenzu, A., Klose, S., Greiner, J., et al. 2012, A&A, 548, A101

Norris, J. P., & Bonnell, J. T. 2006, ApJ, 643, 266

Norris, J. P., Gehrels, N., & Scargle, J. D. 2010, ApJ, 717, 411

Nysewander, M., Fruchter, A. S., & Pe'er, A. 2009, ApJ, 701, 824

Perley, D. A., Kislak, M., & Ganeshalingam, M. 2009, GRB Coordinates Network, 9372

Pian, E., D'Avanzo, P., Benetti, S., et al. 2017, Nature, 551, 67

Planck Collaboration, Ade, P. A. R., Aghanim, N., et al. 2016, A&A, 594, A13

Poole, T. S., & Troja, E. 2006, GRB Coordinates Network, 5069

Price, P. A., Berger, E., Fox, D. B., Cenko, S. B., & Rau, A. 2006, GRB Coordinates Network, 5077

Rosswog, S. 2005, ApJ, 634, 1202

Rosswog, S., Ramirez-Ruiz, E., & Davies, M. B. 2003, MNRAS, 345, 1077

Rosswog, S., Thielemann, F. K., Davies, M. B., Benz, W., & Piran, T. 1998, in Nuclear Astrophysics, ed. W. Hillebrandt & E. Muller, 103

Rowlinson, A., Wiersema, K., Levan, A. J., et al. 2010, MNRAS, 408, 383

Rumyantsev, V., Karimov, R., Salyamov, R., et al. 2006, GRB Coordinates Network, 5184

Rumyantsev, V., Shakhovkoy, D., & Pozanenko, A. 2010, GRB Coordinates Network, Circular Service, No. 10456, #1 (2010), 10456

Ryan, G., van Eerten, H., MacFadyen, A., & Zhang, B.-B. 2015, ApJ, 799, 3

Sari, R., Piran, T., & Narayan, R. 1998, ApJL, 497, L17

Savchenko, V., Ferrigno, C., Kuulkers, E., Author, A. N., & Author, A. N.and Author, A. N. 2017, ApJ

Schlafly, E. F., & Finkbeiner, D. P. 2011, ApJ, 737, 103

Siegel, M. H., & Beardmore, A. P. 2009, GRB Coordinates Network, 9369

Smartt, S. J., Chen, T.-W., Jerkstrand, A., et al. 2017, Nature, 551, 75

Soares-Santos, M., Holz, D. E., Annis, J., et al. 2017, ApJL, 848, L16

Stratta, G., D'Avanzo, P., Piranomonte, S., et al. 2007, A&A, 474, 827

Tanvir, N. R., Levan, A. J., Fruchter, A. S., et al. 2013, Nature, 500, 547

—. 2015, GRB Coordinates Network, Circular Service, No. 18100, #1 (2015), 18100

Tanvir, N. R., Levan, A. J., González-Fernández, C., et al. 2017, ApJL, 848, L27

Tauris, T. M., Kramer, M., Freire, P. C. C., et al. 2017, ApJ, 846, 170

Thielemann, F.-K., Arcones, A., Käppeli, R., et al. 2011, Progress in Particle and Nuclear Physics, 66, 346

Troja, E., Sakamoto, T., Cenko, S. B., et al. 2016a, ApJ, 827, 102

Troja, E., Tanvir, N., Cenko, S. B., et al. 2016b, GRB Coordinates Network, Circular Service, No. 20222, #1 (2016), 20222

Troja, E., Butler, N., Watson, A. M., et al. 2017, GRB Coordinates Network, Circular Service, No. 21051, #1 (2017), 21051

Tunnicliffe, R. L., Levan, A. J., Tanvir, N. R., et al. 2014, MNRAS, 437, 1495

Updike, A. C., Bryngelson, G., & Milne, P. A. 2009, GRB Coordinates Network, 9361

Villar, V. A., Guillochon, J., Berger, E., et al. 2017, ApJL, 851, L21

von Kienlin, A., Meegan, C., Goldstein, A., et al. 2017, GRB Coordinates Network, 21520

Yang, B., Jin, Z.-P., Li, X., et al. 2015, Nature Communications, 6, 7323